



## Research Article

# Bayesian computational methods for estimation of q-Weibull distribution

Ibrahim SADOK<sup>1,\*</sup>

<sup>1</sup>Department of Mathematics and Computer Science, Faculty of Exact Sciences, University of Bechar, Bechar, 08000, Algeria, Laboratory of Mathematics, Djillali Liabes University of Sidi Bel-Abbès, P. O. Box 89, 22000, Sidi Bel-Abbès, Algeria

## ARTICLE INFO

### Article history

Received: 17 October 2024

Revised: 02 January 2025

Accepted: 13 February 2025

### Keywords:

Bayesian Inference; Metropolis-Hastings Algorithm; MLE; Parameter Estimation; Reliability Analysis; Q-Weibull Distribution

## ABSTRACT

The  $q$ -Weibull distribution is a flexible probability distribution that is commonly used in reliability analysis, survival analysis, and extreme value modelling. Obtaining accurate parameter estimates is essential for these applications. This paper investigates several estimation techniques for the  $q$ -Weibull distribution, with special emphasis on the Metropolis–Hastings algorithm. Through an extensive simulation study, we evaluate the performance of these methods across different sample sizes. In addition, we apply them to a real dataset to illustrate their practical utility and to highlight situations where the Metropolis–Hastings approach proves particularly advantageous.

**Cite this article as:** Sadok I. Bayesian computational methods for estimation of  $q$ -Weibull distribution. Sigma J Eng Nat Sci 2026;44(2):1094–1110.

## INTRODUCTION

The Weibull distribution has served as a workhorse in reliability analysis across many disciplines. In medicine, the Weibull distribution is often used to estimate survival times for cancer patients, helping researchers better understand treatment effectiveness and expected life spans [1]. In engineering, it plays an important role in predicting the fatigue life of mechanical components that are exposed to repeated or cyclic stresses [2]. It is also widely applied in the wind energy field, where it helps describe extreme wind speeds for turbine design and risk evaluation [3]. In finance, analysts use it to model stock price variations and capture rare but significant market events [4]. Moreover, in image processing, the Weibull distribution can be useful for modeling different types of noise patterns [5].

The classical Weibull distribution has the following probability density function (pdf):

$$f(x|k, \lambda) = \frac{k}{\lambda} \left(\frac{x}{\lambda}\right)^{k-1} e^{-(x/\lambda)^k}, \quad (1)$$

where  $k > 0$  denotes the shape parameter, and  $\lambda > 0$  represents the scale parameter. This formulation describes the distribution using two parameters, which together provide a high degree of flexibility in modeling different types of data, particularly in applications involving failure times and survival analysis.

Equation (1) can be interpreted as a generalization of the exponential distribution, since it reduces to the exponential case when the shape parameter  $k = 1$ . One of the main reasons for the widespread use of the Weibull distribution is its ability to capture the behavior of many

### \*Corresponding author.

\*E-mail address: [ibrahim.sadok@univ-bechar.dz](mailto:ibrahim.sadok@univ-bechar.dz)

This paper was recommended for publication in revised form by Editor-in-Chief Ahmet Selim Dalkilic



real-world systems. In practice, such systems often exhibit a relatively high probability of failure at early stages, followed by a decreasing failure rate over time [6]. For this reason, the Weibull distribution has become a standard tool in reliability engineering and survival analysis.

However, its broad applicability, the classical Weibull distribution may not adequately describe data with heavy tails or complex, non-extensive behavior. To overcome these limitations, several generalized forms have been proposed. Among them, a notable extension is based on the  $q$ -exponential function, leading to the so-called  $q$ -Weibull distribution [7–9].

The  $q$ -exponential function, which generalizes the classical exponential function, is defined:

$$e_q(x) = [1 + (1 - q)x]^{1/(1-q)}, \quad (2)$$

where  $x \in \mathbb{R}$  and  $q$  determines the level of non-extensive behavior in the model. When  $q = 1$ , the  $q$ -exponential function reduces to the traditional exponential function [10]. The  $q$ -exponential definition incorporates a cut-off criterion that effectively precludes negative or complex values, a critical attribute when associating the function with probabilities. Notably, for select parameter values, the  $q$ -exponential displays a transition between an exponential profile and a power-law regime [11, 12]. More specifically, when  $a > 0$  and  $q > 1$ ,  $e_q(2ax)$  exhibits power-law behavior for large values of  $x$ , leading to heavy-tailed distributions..

The  $q$ -Weibull distribution provides greater flexibility and adaptability, particularly in datasets characterized by power-law behaviour or non-extensive statistics. This generalized form has been applied to diverse areas, such as dielectric breakdown modelling in electronic devices [13] and financial market volatility analysis [14]. Recent applications in environmental sciences further demonstrate the relevance of distribution in capturing extreme weather events and modelling climate change and flood data .

In this article, we introduce a Bayesian approach for parameter estimation in the context of the  $q$ -Weibull distribution. The estimation procedure relies on Markov Chain Monte Carlo (MCMC) techniques, where Gibbs sampling is used to iteratively update the parameters of the distribution. In recent years, advances in Markov Chain Monte Carlo (MCMC) methods, including adaptive algorithms [15, 16] and variational inference techniques [17], have significantly improved both convergence properties and computational efficiency. In this study, particular attention is given to the Metropolis–Hastings algorithm [18] and two of its widely used variants: the Independent Metropolis–Hastings (IMH) and the Random Walk Metropolis (RWM) algorithms [19].

Bayesian estimation methods, as considered in this work, offer several advantages in practical applications such as engineering reliability and survival analysis. In particular, their ability to incorporate prior information and

to explicitly account for uncertainty makes them especially valuable when dealing with complex real-world data.

This study provides a comparative analysis of maximum likelihood estimation (MLE) and Bayesian approaches (specifically IMH and RWM) for estimating the parameters of the  $q$ -Weibull distribution. Although the  $q$ -Weibull model is recognized for its flexibility in capturing diverse data behaviors, the issue of reliable parameter estimation has not yet been thoroughly investigated. Through an extensive simulation study covering different sample sizes, the performance of MLE, IMH, and RWM is examined. The results indicate that the RWM approach provides improved performance compared with standard MCMC implementations when estimating posterior distributions. In addition, the study illustrates the usefulness of Bayesian methods through applications to real datasets, emphasizing their relevance in fields such as engineering and the natural sciences.

The practical importance of this work lies in the flexibility of the  $q$ -Weibull distribution for modelling a wide range of phenomena. In engineering, it is commonly used in reliability analysis, for instance, to model material fatigue under varying stress conditions. In the natural sciences, the distribution is well suited for survival modelling and extreme-value analysis, where classical models often struggle to capture tail behaviour. Moreover, the comparative assessment of estimation techniques (particularly the advantages of Bayesian methods such as IMH and RWM) offers useful guidance for researchers and practitioners working with complex and heterogeneous datasets.

The subsequent sections of this paper are structured as follows. Section 2 introduces the  $q$ -Weibull model and delineates its characteristic statistics. Section 3 presents the frequentist analysis of the  $q$ -Weibull distribution, where the parameters are estimated using the MLE and the corresponding confidence intervals are derived. Section 4 then introduces the Bayesian framework developed for parameter estimation. We elucidate the resampling procedures employing both IMH and RWM algorithms. Section 5 presents a comprehensive simulation study. Section 6 demonstrates the practical application of the proposed methods through the analysis of two real-world datasets. Finally, Section 7 summarizes the main findings of the study.

## BACKGROUND

The  $q$ -Weibull model is derived by replacing the exponential function in the classical Weibull model (represented by equation (1)) with a  $q$ -exponential. A detailed explanation of this substitution can be found in [13]. The resulting expression for the  $q$ -Weibull pdf is given by

$$f_q(x|q, k, \lambda) = (2 - q) \frac{k}{\lambda} \left(\frac{x}{\lambda}\right)^{k-1} e_q\left(-\left(\frac{x}{\lambda}\right)^k\right), \quad (3)$$

where  $k > 0$  and  $q < 2$  are shape parameters, and  $\lambda > 0$  is a scale parameter.

By substituting the  $q$ -exponential function  $e_q(x)$  into equation (3), we can rewrite the pdf of the  $q$ -Weibull distribution as follows:

$$f_q(x|q, k, \lambda) = (2 - q) \frac{k}{\lambda^k} x^{k-1} \left[ 1 - (1 - q) \left( \frac{x}{\lambda} \right)^k \right]^{\frac{1}{1-q}}$$

where the domain of the  $q$ -Weibull distribution is given by the following piecewise function:

$$x \in \begin{cases} [0, +\infty) & 1 < q < 2 \\ [0, \lambda(1 - q)^{-1/k}] & q < 1 \end{cases}$$

As the parameter  $q \rightarrow 1$ , the function  $f_q$  transforms into the Weibull pdf (1). When  $k$  is set to 1, it corresponds to the

$q$ -exponential pdf (2). Moreover, when both  $q$  and  $k$  tend towards 1, it transitions into the exponential distribution.

Consider a random sample, denoted as  $x = (x_1, x_2, \dots, x_n)$ , drawn from the  $q$ -Weibull distribution. The likelihood function for  $(q, k, \lambda)$  given  $x$ , takes the form

$$L(q, k, \lambda|x) = \prod_{i=1}^n f_q(x_i|q, k, \lambda) = \prod_{i=1}^n (2 - q) \frac{k}{\lambda^k} x_i^{k-1} \left[ 1 - (1 - q) \left( \frac{x_i}{\lambda} \right)^k \right]^{\frac{1}{1-q}} \quad (4)$$

Figure 1 illustrates density curves for the  $q$ -Weibull distribution, highlighting the effects of varying parameters  $q$ ,  $k$ , and  $\lambda$ . In the first set of curves,  $k = 2$  and  $\lambda = 1$  are held constant, while  $q$  varies from 0.1 to 1. This clearly shows how the parameter  $q$  affects the tail behaviour: smaller values of  $q$  lead to heavier tails, indicating greater dispersion in the data. In the second set,  $q = 0.5$  and  $\lambda = 1$  are fixed while

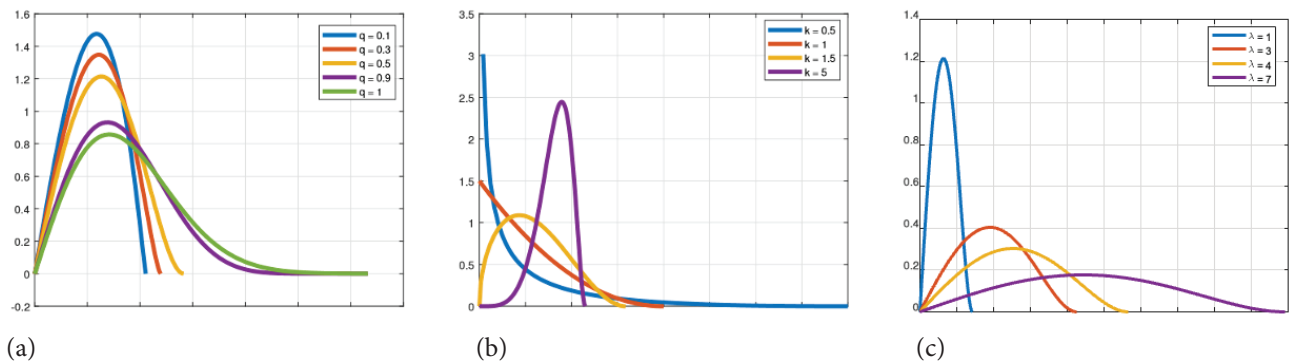


**Figure 1.**  $q$ -Weibull probability density function with reference parameters  $q = 0.5, k = 2, \lambda = 1$  with changing: (a) parameter  $q$ , (b) shape parameter  $k$ , (c) scale parameter  $\lambda$ .

**Table 1.** Statistical characteristics of the  $q$ -Weibull Distribution for  $q < 1$ .

Characteristics	Functional form
pdf	$(2 - q) \frac{k}{\lambda^k} x^{k-1} \left[ 1 - (1 - q) \left( \frac{x}{\lambda} \right)^k \right]^{\frac{1}{1-q}}$
cdf	$1 - \left[ 1 - (1 - q) \left( \frac{x}{\lambda} \right)^k \right]^{\frac{2-q}{1-q}}; 0 \leq x \leq \lambda(1 - q)^{-1/k}$
hrf	$\frac{k(2 - q)x^{k-1}}{\lambda^k \left[ 1 - (1 - q) \left( \frac{x}{\lambda} \right)^k \right]};  x  < \lambda(1 - q)^{-1/k}$
$s^{\text{th}}$ moment	$\frac{\lambda^s(2 - q)}{(1 - q)^{1+s/k}} B\left(\frac{s}{k} + 1, \frac{2 - q}{1 - q}\right)$
Mean	$\frac{\lambda(2 - q)}{(1 - q)^{1+1/k}} B\left(\frac{1}{k} + 1, \frac{2 - q}{1 - q}\right)$
Variance	$\frac{\lambda^2(2 - q)}{(1 - q)^{1+2/k}} \left[ B\left(\frac{2}{k} + 1, \frac{2 - q}{1 - q}\right) - \frac{2 - q}{1 - q} B^2\left(\frac{1}{k} + 1, \frac{2 - q}{1 - q}\right) \right]$
Mode	$\lambda \left[ \frac{k-1}{k+(k-1)(1-q)} \right]^{\frac{1}{k}}; k > 0$

**Table 2.** Statistical Characteristics of the  $q$ -Weibull Distribution for  $1 < q < 2$ .

Characteristics	Functional form
pdf	$(2 - q) \frac{k}{\lambda^k} x^{k-1} \left[ 1 + (1 - q) \left( \frac{x}{\lambda} \right)^k \right]^{\frac{1}{1-q}}$
cdf	$1 - \left[ 1 + (1 - q) \left( \frac{x}{\lambda} \right)^k \right]^{\frac{2-q}{1-q}}; x > 0$
hrf	$\frac{k(2 - q)x^{k-1}}{\lambda^k \left[ 1 + (1 - q) \left( \frac{x}{\lambda} \right)^k \right]}$
$s^{\text{th}}$ moment	$\frac{\lambda^s(2 - q)}{(1 - q)^{1+s/k}} B \left( \frac{s}{k} + 1, \frac{1}{q-1} - \frac{s}{k} - 1 \right)$
Mean	$\frac{\lambda(2 - q)}{(1 - q)^{1+1/k}} B \left( \frac{1}{k} + 1, \frac{1}{q-1} - \frac{1}{k} - 1 \right)$
Variance	$\frac{\lambda^2(2 - q)}{(1 - q)^{1+2/k}} \left[ B \left( \frac{2}{k} + 1, \frac{1}{q-1} - \frac{2}{k} - 1 \right) + \frac{2 - q}{1 - q} B^2 \left( \frac{1}{k} + 1, \frac{1}{q-1} - \frac{1}{k} - 1 \right) \right]$
Mode	$\lambda \left[ \frac{k-1}{k-(k-1)(1-q)} \right]^{\frac{1}{k}}; k > 0$

$k$  ranges from 0.5 to 5. Here, we see that  $k$  mainly controls the shape and the height of the peak, with larger values producing sharper and more pronounced peaks. In the third set of curves,  $q = 0.5$  and  $k = 1$  are kept constant, and  $\lambda$  varies from 1 to 7. This highlights its role as a scale parameter, shifting the distribution along the horizontal axis. The significance of studying the  $q$ -Weibull distribution lies in its ability to generate diverse density curves by varying parameters  $q$ ,  $k$ , and  $\lambda$ , which influence tail behaviour, shape, and scale, respectively. This flexibility enables the modelling of various data types, from light-tailed to heavy-tailed distributions. These characterisations allows for a clear visualization of how changes in each parameter impact the distribution's behaviour, making these relationships more intuitive and accessible.

Tables 1 and 2 present a detailed summary of the main statistical properties of the  $q$ -Weibull distribution for the cases  $q < 1$  and  $1 < q < 2$ , respectively. Each table lists the probability density function (pdf), cumulative distribution function (cdf), hazard rate function (hrf), the  $s^{\text{th}}$  moment, mean, variance, and mode, along with their corresponding mathematical formulas. Additionally, the tables reference the beta function  $B(x, y)$ , defined as:

$$B(x, y) = \int_0^1 t^{x-1} (1 - t)^{y-1} dt$$

This information collectively offers a detailed insight into the behaviour and properties of the  $q$ -Weibull distribution for cases  $q < 1$  and  $1 < q < 2$ .

## FREQUENTIST ANALYSIS OF THE $q$ -WEIBULL DISTRIBUTION

### Maximum Likelihood Estimates of the $q$ -Weibull Distribution Parameters

In engineering applications, the primary challenge lies in the estimation of the  $q$ -Weibull parameters. Among the available methods for estimating  $q$ -Weibull distribution parameters, the most commonly used one is the MLE [11]. However, it is important to note that the first derivatives of the log-likelihood function with respect to the parameters are non-linear, making it extremely challenging to derive analytical solutions.

The logarithm of the likelihood function for this sample, which quantifies the probability of observing these values in the given distribution, can be expressed as follows:

$$\begin{aligned} \ln L(q, k, \lambda | x) = & n \ln(2 - q) + n \ln k - k n \ln \lambda + (k - 1) \sum_{i=1}^n \ln(x_i) \\ & + \frac{1}{1 - q} \sum_{i=1}^n \ln \left[ 1 - (1 - q) \left( \frac{x_i}{\lambda} \right)^k \right]. \end{aligned} \tag{6}$$

The partial derivatives of the log-likelihood function concerning the parameters  $q$ ,  $k$ , and  $\lambda$  are as follows:

$$\begin{aligned} \frac{\partial \ln L(q, k, \lambda | x)}{\partial q} &= \frac{n}{2-q} + \frac{1}{(1-q)} \sum_{i=1}^n \frac{x_i^k}{\lambda^k - (1-q)x_i^k} \\ &\quad + \frac{1}{(1-q)^2} \sum_{i=1}^n \ln \left[ 1 - (1-q) \left( \frac{x_i}{\lambda} \right)^k \right], \\ \frac{\partial \ln L(q, k, \lambda | x)}{\partial k} &= \frac{n}{k} - n \ln \lambda + \sum_{i=1}^n x_i - \sum_{i=1}^n \frac{x_i^k \ln \left( \frac{x_i}{\lambda} \right)}{\lambda^k - (1-q)x_i^k}, \\ \frac{\partial \ln L(q, k, \lambda | x)}{\partial \lambda} &= -\frac{k}{\lambda} \left( n - \sum_{i=1}^n \frac{x_i^k}{\lambda^k - (1-q)x_i^k} \right). \end{aligned}$$

Because of the non-linearity of these derivatives, obtaining closed-form solutions for the MLEs, namely  $\hat{q}$ ,  $\hat{k}$ , and  $\hat{\lambda}$  is a formidable task. To tackle this challenge, a constrained optimization problem is formulated, seeking to maximize the natural logarithm of the likelihood function  $\ln L$  given by equation (6) while satisfying the conditions  $q < 2$ ,  $k > 0$ , and  $\lambda > 0$ .

The  $q$ -Weibull model indeed poses a disadvantage due to the complexity of parameter estimation. Given the intricacies of the calculation process and the substantial computational requirements for each method, we have resorted to the Newton–Raphson method to obtain the optimal parameters. This approach reduces the challenges of estimating the  $q$ -Weibull parameters, leading to more accurate results in engineering applications.

**Confidence Intervals for the  $q$ -Weibull Parameters**

In this section, we focus on constructing confidence intervals (CIs) for both the  $q$ -Weibull parameters and the reliability parameters, based on the asymptotic normality property of maximum likelihood estimators (MLEs). To achieve this, we frequently turn to the Fisher information matrix, a valuable tool in establishing CIs for parameters when capitalizing on the asymptotic normality of the MLEs.

In this context, let us consider the parameter of interest, referred to as  $\Theta$ . Under specified regularity conditions, it can be observed that the MLEs  $\hat{\Theta}$  approximate a normal distribution  $\mathcal{N}(\Theta, I^{-1}(\Theta))$  as the sample size  $n \rightarrow \infty$ . Here,  $I^{-1}(\Theta)$  represents the inverse matrix derived from the Fisher information matrix. Notably, the components of the Fisher information matrix are directly linked to the expected values of the second-order derivatives of  $\ln L$ , as exemplified in equation (6). This matrix is expressed as

$$I(q, k, \lambda) = -\mathbb{E} \begin{bmatrix} \frac{\partial^2 \ln L(q, k, \lambda | x)}{\partial q^2} & \frac{\partial^2 \ln L(q, k, \lambda | x)}{\partial q \partial k} & \frac{\partial^2 \ln L(q, k, \lambda | x)}{\partial q \partial \lambda} \\ \frac{\partial^2 \ln L(q, k, \lambda | x)}{\partial k \partial q} & \frac{\partial^2 \ln L(q, k, \lambda | x)}{\partial k^2} & \frac{\partial^2 \ln L(q, k, \lambda | x)}{\partial k \partial \lambda} \\ \frac{\partial^2 \ln L(q, k, \lambda | x)}{\partial \lambda \partial q} & \frac{\partial^2 \ln L(q, k, \lambda | x)}{\partial \lambda \partial k} & \frac{\partial^2 \ln L(q, k, \lambda | x)}{\partial \lambda^2} \end{bmatrix}.$$

A previous study conducted in [20–28] utilized this approximation to determine the confidence intervals for the  $q$ -Weibull parameters. In this context, we will perform the derivation of the expected values. When calculating the

expected values becomes a challenging task, an alternative approach is to estimate them by using the negations of the second-order derivatives of  $\ln L$  evaluated at the MLEs [5, 27]. The second-order derivatives of the natural logarithm of the likelihood function are as follows

$$\begin{aligned} \frac{\partial^2 \ln L(q, k, \lambda | x)}{\partial q^2} &= -\frac{n}{(2-q)^2} - \frac{1}{1-q} \sum_{i=1}^n \frac{x_i^{2k}}{(\lambda^k - (1-q)x_i^k)^2} \\ &\quad + \frac{2}{(1-q)^2} \sum_{i=1}^n \frac{x_i^k}{\lambda^k - (1-q)x_i^k} \\ &\quad + \frac{2}{(1-q)^3} \sum_{i=1}^n \ln \left[ 1 - (1-q) \left( \frac{x_i}{\lambda} \right)^k \right], \\ \frac{\partial^2 \ln L(q, k, \lambda | x)}{\partial q \partial k} &= \frac{\partial^2 \ln L(q, k, \lambda | x)}{\partial k \partial q} = \sum_{i=1}^n \frac{x_i^{2k} \ln \left( \frac{x_i}{\lambda} \right)}{(\lambda^k - (1-q)x_i^k)^2}, \\ \frac{\partial^2 \ln L(q, k, \lambda | x)}{\partial q \partial \lambda} &= \frac{\partial^2 \ln L(q, k, \lambda | x)}{\partial \lambda \partial q} = -\frac{k}{\lambda} \sum_{i=1}^n \frac{x_i^{2k}}{(\lambda^k - (1-q)x_i^k)^2}, \\ \frac{\partial^2 \ln L(q, k, \lambda | x)}{\partial k^2} &= -\frac{n}{k^2} - \lambda^k \sum_{i=1}^n \frac{x_i^k \ln^2 \left( \frac{x_i}{\lambda} \right)}{(\lambda^k - (1-q)x_i^k)^2}, \\ \frac{\partial^2 \ln L(q, k, \lambda | x)}{\partial k \partial \lambda} &= \frac{\partial^2 \ln L(q, k, \lambda | x)}{\partial \lambda \partial k} = -\frac{1}{\lambda} \left( n - \sum_{i=1}^n \frac{x_i^k}{\lambda^k - (1-q)x_i^k} \right) \\ &\quad + k \lambda^{k-1} \sum_{i=1}^n \frac{x_i^k \ln(x_i/\lambda)}{(\lambda^k - (1-q)x_i^k)^2}, \\ \frac{\partial^2 \ln L(q, k, \lambda | x)}{\partial \lambda^2} &= \frac{k}{\lambda^2} \left( n - \sum_{i=1}^n \frac{x_i^k}{\lambda^k - (1-q)x_i^k} \right) \\ &\quad - k^2 \lambda^{k-2} \sum_{i=1}^n \frac{x_i^k}{(\lambda^k - (1-q)x_i^k)^2}. \end{aligned}$$

The covariance matrix for the MLEs of the  $q$ -Weibull distribution parameters can be estimated by taking the inverse of the observed information matrix  $I(q, k, \lambda)$ . This covariance matrix is also equivalent to the inverse of the Fisher information matrix, which is

$$Cov(q, k, \lambda) = I^{-1}(q, k, \lambda) = \begin{bmatrix} var_{11} & cov_{12} & cov_{13} \\ cov_{21} & var_{22} & cov_{23} \\ cov_{31} & cov_{32} & var_{33} \end{bmatrix}.$$

After obtaining the covariance matrix, we can proceed to construct asymptotic confidence intervals for the  $q$ -Weibull distribution parameters. These intervals provide an estimate of the parameter values with a  $(1 - \alpha)100\%$  level of confidence. The following are the asymptotic confidence intervals for the parameters  $q$ ,  $k$ , and  $\lambda$ :

$$\begin{aligned} CI[q: (1 - \alpha)100\%] &= \left[ \hat{q} + z_{\frac{\alpha}{2}} \sqrt{var_{11}}, \hat{q} + z_{1-\frac{\alpha}{2}} \sqrt{var_{11}} \right], \\ CI[k: (1 - \alpha)100\%] &= \left[ \hat{k} + z_{\frac{\alpha}{2}} \sqrt{var_{22}}, \hat{k} + z_{1-\frac{\alpha}{2}} \sqrt{var_{22}} \right], \\ CI[\lambda: (1 - \alpha)100\%] &= \left[ \hat{\lambda} + z_{\frac{\alpha}{2}} \sqrt{var_{33}}, \hat{\lambda} + z_{1-\frac{\alpha}{2}} \sqrt{var_{33}} \right]. \end{aligned}$$

In this context,  $\hat{q}$ ,  $\hat{k}$ , and  $\hat{\lambda}$  represent the ML estimators of the parameters. Meanwhile,  $Z_{\frac{\alpha}{2}}$  and  $Z_{1-\frac{\alpha}{2}}$  correspond to the  $\frac{\alpha}{2}$  and  $1 - \frac{\alpha}{2}$  quantiles of the standard normal distribution, respectively. While  $var_{11}$ ,  $var_{22}$ , and  $var_{33}$  correspond to the diagonal elements of the covariance matrix  $Cov(q, k, \lambda)$ .

### BAYESIAN ANALYSIS OF THE $q$ -WEIBULL DISTRIBUTION

In this section, we outline the Bayesian approach to estimate the parameters of the  $q$ -Weibull distribution. To begin, we assume that the prior distributions for the parameters  $(q, k, \lambda)$  are independent, meaning we can express the joint prior as the product of individual priors [21], i.e.  $\pi(q, k, \lambda) = \pi(q)\pi(k)\pi(\lambda)$ .

The main objective is to estimate the Bayesian values of the parameters:  $q$ ,  $k$ , and  $\lambda$ . To proceed, we assign suitable prior distributions to each parameter according to their nature.

- For the shape parameter  $q$ , we consider a Beta prior, written as  $\pi(q) = \text{Beta}(q|q_1, q_2)$ , where  $q_1$  and  $q_2$  are known hyper-parameters. This choice is natural since the Beta distribution is defined on the interval  $[0,1]$ , which coincides with the admissible range of  $q$ .
- For the parameter  $k$ , we use a Gamma prior, denoted by  $\pi(k) = \Gamma(k|k_1, k_2)$ , with  $k_1$  and  $k_2$  are known hyperparameters. The Gamma distribution is versatile and can accommodate a wide range of shapes, making it a common choice for modelling  $k$ .
- Similarly, for the scale parameter  $\lambda$ , we assign a prior distribution, and the Gamma distribution is a popular choice, represented as  $\pi(\lambda) = \Gamma(\lambda|\lambda_1, \lambda_2)$ , with known hyper-parameters  $\lambda_1$  and  $\lambda_2$ . The Gamma distribution is highly flexible and can accommodate a wide range of shapes, making it suitable for modeling positive parameters. It is also commonly used for scale-type parameters such as  $\lambda$ .

**Remark:** The hyperparameters of the priors are selected to balance computational convenience with limited prior influence. In particular, a Beta (1,1) prior is adopted for  $q$ , corresponding to a uniform distribution on  $[0,1]$ , which reflects the absence of strong prior information. For  $k$  and  $\lambda$ ,  $\Gamma(0.1,0.1)$  priors were chosen to provide sufficient variance for robust parameter exploration. A sensitivity analysis, varying these hyper-parameters (e.g., Beta (0.5, 2) for  $q$  and  $\Gamma(1,1)$  for  $k$  and  $\lambda$ ), demonstrated that posterior estimates remained stable across the tested ranges, confirming the reliability of the chosen priors.

Using the Bayes theorem, the joint posterior distribution for  $(q, k, \lambda)$  upon which inference is based, is given by

$$\pi(q, k, \lambda|x) \propto L(q, k, \lambda|x)\pi(q)\pi(k)\pi(\lambda),$$

where  $L(q, k, \lambda|x)$  is defined in equation (6).

The conditional posterior distributions are

$$\begin{aligned} q|x, k, \lambda &\propto (2-q)^n \exp\left(\sum_{i=1}^n \frac{1}{1-q} \ln\left[1 - (1-q)\left(\frac{x_i}{\lambda}\right)^k\right]\right) q^{q_1-1} (1-q)^{q_2-1}, \\ k|x, q, \lambda &\propto \frac{k^{n+k_1-1}}{\lambda^{kn}} e^{-kk_2} \exp\left(\sum_{i=1}^n (k-1)\ln(x_i) + \frac{1}{1-q} \ln\left[1 - (1-q)\left(\frac{x_i}{\lambda}\right)^k\right]\right), \\ \lambda|x, q, k &\propto \lambda^{\lambda_1-nk-1} e^{-\lambda k_2} \exp\left(\sum_{i=1}^n \frac{1}{1-q} \ln\left[1 - (1-q)\left(\frac{x_i}{\lambda}\right)^k\right]\right). \end{aligned}$$

The complexity of the posterior distribution precludes the derivation of closed-form expressions for its properties. Consequently, our approach is to employ Markov chain Monte Carlo (MCMC) methods to obtain samples from this distribution, facilitating the extraction of parameter inferences.

Yet, the conditional posterior distribution for the parameters  $q, k, \lambda$  does not conform to any readily available closed distribution, and its resampling procedure is not straightforward. In such instances, the conventional Bayesian approach involves the utilization of the Metropolis-Hastings algorithm.

#### Metropolis-Hastings Algorithm

The Metropolis-Hastings (MH) algorithm represents the most widely recognized instances of MCMC techniques. This algorithm is employed to generate samples from arbitrary distributions for which we lack a direct method for generating random samples. In a manner analogous to acceptance-rejection sampling, the MH algorithm posits that at each iteration of the process, a potential value can be drawn from a proposal distribution.

Consequently, the candidate value is accepted or rejected during each iteration, contingent upon the calculation of an appropriate acceptance probability. This iterative process is essential for steering the Markov chain toward the target distribution, making it an effective method for sampling from complex models. For a more detailed explanation of the Metropolis-Hastings algorithm, readers are referred to the foundational works [21–23].

To update parameter  $q$  using the Metropolis-Hastings algorithm, suppose that  $(q, k, \lambda)$  represents the current state of the Markov chain. Let  $q^*$  be a candidate value generated from a proposal density denoted as  $g(q^*|q)$ . The value  $q^*$  is then accepted with a probability denoted as  $\Psi(q^*|q) = \min(1, A_q)$ , where  $A_q$  is defined as

$$A_q = \frac{L(q^*, k, \lambda)\pi(q^*)g(q|q^*)}{L(q, k, \lambda)\pi(q)g(q^*|q)}, \tag{7}$$

where  $L(\cdot|y)$  represents the likelihood function, as described in equation (4).

In a practical context, the MH algorithm is executed as outlined below

**Algorithm 1:** Metropolis-Hastings Algorithm

1: **Initialization:** Initialize the iteration count  $l = 1$  and set the initial state as:  $(q^{(l-1)}, k^{(l)}, \lambda^{(l)})$

2: **While**  $l \leq L$

**Step 1:** Generate a proposal state  $q^* \sim g(q^*|q^{(l-1)})$ .

**Step 2:** Calculate acceptance probability  $\Psi(q^*|q^{(l-1)}) = \min(1, A_q)$ ,

where  $A_q$  is given in equation (7);

**Step 3:** Generate a random number  $u \sim \mathcal{U}(0,1)$

**If**  $u \leq \Psi(q^*|q^{(l-1)})$

Accept  $q^*$  and set  $q^{(l)} = q^*$  **else**

Reject  $q^*$  and set  $q^{(l)} = q^{(l-1)}$

**end While**

**Two Typical Selections for  $g(\cdot)$** 

To effectively implement the MH algorithm, it is essential to define the candidate-generating density  $g(q^*|q)$ . Typically,  $g(\cdot)$  is selected to ensure it allows for straightforward sampling. In the following section, we elaborate on two commonly utilized choices for  $g(\cdot)$ .

- *Independent Metropolis-Hastings (IMH):* When  $g(q^*|q) = g(q^*)$ , meaning that the candidate-generating density is independent of the current value, we obtain a special case of the original algorithm. In this simplified scenario, the expression for  $A_q$  becomes

$$A_q = \frac{L(q^*, k, \lambda)\pi(q^*)}{L(q, k, \lambda)\pi(q)} \frac{g(q)}{g(q^*)}$$

To address this situation, one can configure  $g(q^*)$  to be the prior distribution, denoted as  $g(q^*) = \pi(q^*)$ . Consequently, the expression for  $A_q$  can be derived by considering the likelihood ratio

$$A_q = \frac{L(q^*, k, \lambda)}{L(q, k, \lambda)}. \quad (8)$$

The implementation of this algorithm is detailed in the following manner.

**Algorithm 2:** Independent Metropolis-Hastings algorithm

1: **Initialization:** Initialize the iteration count  $l = 1$  and set the initial state as:  $(q^{(l-1)}, k^{(l)}, \lambda^{(l)})$

2: **While**  $l \leq L$

**Step 1:** Generate a proposal state  $q^* \sim \text{Beta}(q_1, q_2)$

**Step 2:** Calculate acceptance probability  $\Psi(q^*|q^{(l-1)}) = \min(1, A_q)$ ,

where  $A_q$  is given in (8);

**Step 3:** Generate a random number  $u \sim \mathcal{U}(0,1)$

**If**  $u \leq \Psi(q^*|q^{(l-1)})$

Accept  $q^*$  and set  $q^{(l)} = q^*$  **else**

Reject  $q^*$  and set  $q^{(l)} = q^{(l-1)}$

**end While**

- *Random Walk Metropolis (RWM):* When the candidate generating-density, denoted as  $g(q^*|q)$ , exhibits symmetry and the likelihood of transitioning from state  $q$  to  $q^*$  depends solely on the distance between them, that is,  $g(q^*|q) = d(|q-q^*|)$ , with  $d$  representing a symmetric density, the expression for  $A_q$  can be simplified as follows

$$A_q = \frac{L(q^*, k, \lambda)\pi(q^*)}{L(q, k, \lambda)\pi(q)}, \quad (9)$$

While the choice of prior distributions as the candidate generating-density is theoretically elegant, it can lead to numerous rejections of proposed moves, resulting in slow convergence of the algorithm. This issue is particularly pronounced when prior information is unavailable and the prior distribution has a high variance. By employing the RWM method, we can explore the vicinity of the current chain value to propose a new one, offering a more efficient convergence technique.

To implement this approach, we generate a new value  $q^*$  by setting it as  $q^* = q + \varepsilon$ , where  $\varepsilon$  is a random perturbation drawn from a Normal distribution with a mean of 0 and a variance of  $\sigma_q^2$ , represented as  $\varepsilon \sim \mathcal{N}(0, \sigma_q^2)$ . This implies that  $q^* \sim \mathcal{N}(q, \sigma_q^2)$ . The algorithm is implemented as follows

**Algorithm 3:** Random Walk Metropolis algorithm

1: **Initialization:** Initialize the iteration count  $l = 1$  and set the initial state as:  $(q^{(l-1)}, k^{(l)}, \lambda^{(l)})$

2: **While**  $l \leq L$

**Step 1:** Generate  $\varepsilon \sim \mathcal{N}(0, \sigma_q^2)$  and set  $q^* = q^{(l-1)} + \varepsilon$

**Step 2:** Calculate acceptance probability  $\Psi(q^*|q^{(l-1)}) = \min(1, A_q)$ , where  $A_q$  is given in (9);

**Step 3:** Generate a random number  $u \sim \mathcal{U}(0,1)$

**If**  $u \leq \Psi(q^*|q^{(l-1)})$

Accept  $q^*$  and set  $q^{(l)} = q^*$  **else**

Reject  $q^*$  and set  $q^{(l)} = q^{(l-1)}$

**end While**

The parameter  $\sigma_q^2$  plays a crucial role in the RWM algorithm, as it determines the size of the random perturbations added to the current state when proposing new moves in the Markov chain. In other words, it controls the step size of the chain as it explores the state space. Selecting the appropriate value for  $\sigma_q^2$  is of paramount importance because it profoundly influences the efficiency of the MCMC algorithm. This influence operates at both extremes of  $\sigma_q^2$ :

**Small  $\sigma_q^2$ :** When  $\sigma_q^2$  is too small, the random perturbations are minor, resulting in a high acceptance rate for proposed states. While this may seem desirable, it can slow down the exploration of the entire state space because the Markov chain takes small, cautious steps.

Large  $\sigma_q^2$ : on the other hand, if  $\sigma_q^2$  is excessively large, can result in a high rejection rate for proposed states. This can dramatically slow down the convergence of the Markov chain because most steps are rejected, and it takes longer for the chain to explore the space effectively.

Selecting the Right  $\sigma_q^2$  values is a crucial step in the process. The objective, as proposed in [19], is to find a value where the acceptance ratio (the proportion of proposed states that are accepted) falls within a specific range, typically between 20% and 30%. According to these authors, this range strikes a good balance between playing it safe and efficiently getting to the solution.

### SIMULATION STUDY

#### Maximum Likelihood Estimation (MLE) for $q$ -Weibull Distribution Parameters

We conducted a comprehensive Monte Carlo simulation to evaluate the performance of the ML estimators for the  $q$ -Weibull parameters under different settings. The study necessitates specified values for  $q$ ,  $k$  and  $\lambda$ .

For each designated parameter setting, MLEs ( $\hat{q}$ ,  $\hat{k}$ ,  $\hat{\lambda}$ ) are computed from a random sample with the sample size set at 200. This process is replicated 1000 times for each configuration. To gauge the efficacy of the MLEs, metrics such as mean squared error (MSE), Biases<sup>2</sup>, and median absolute error (MedAE) are calculated.

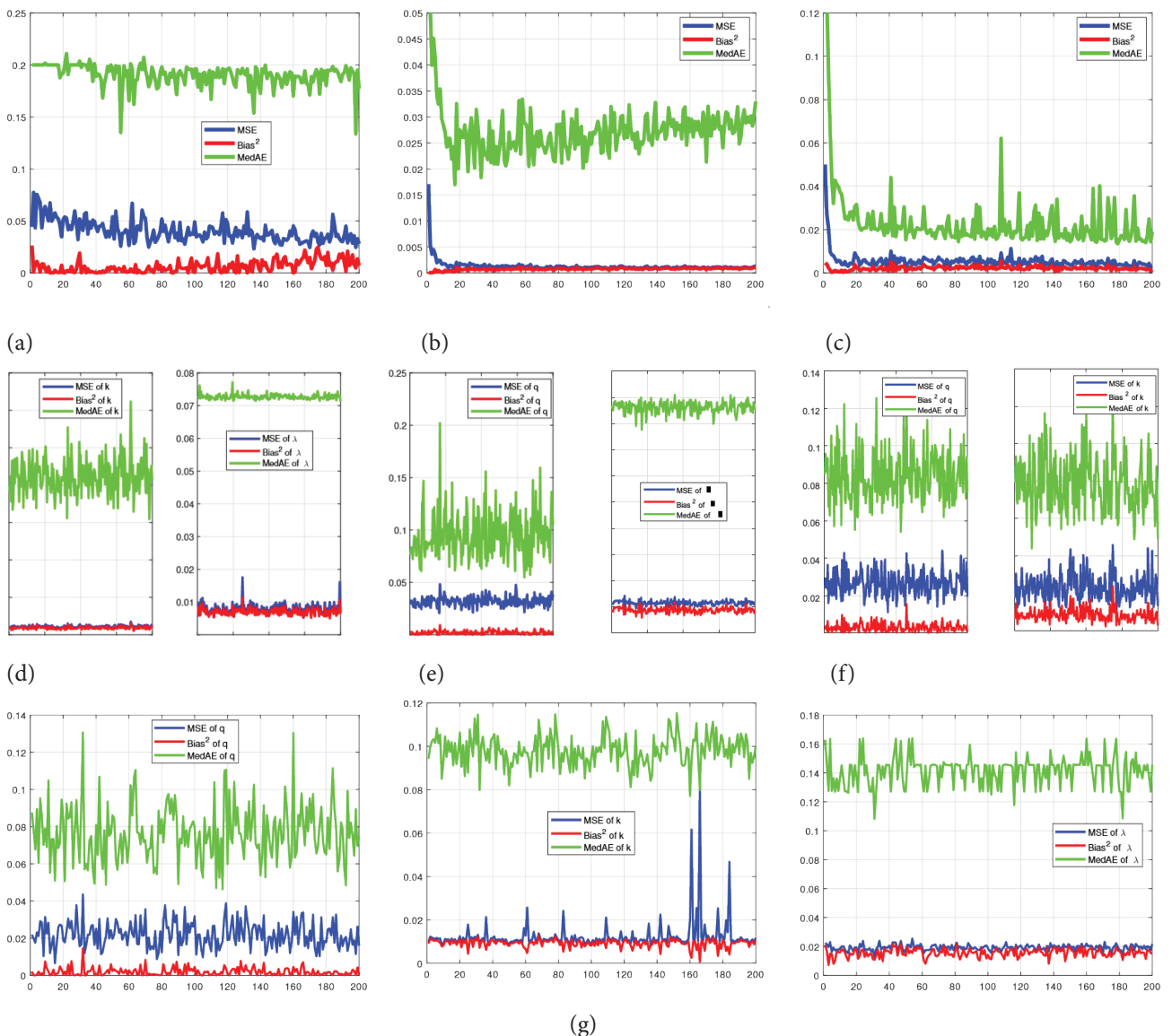


**Figure 2.** Comparison of MSE, Bias<sup>2</sup>, and MedAE for the MLE of the parameters  $q$  (a),  $k$  (b),  $\lambda$  (c),  $(k, \lambda)$  fixed (d),  $(q, \lambda)$  fixed (e),  $(q, k)$  fixed (f),  $(q, k, \lambda)$  non fixed (g), for increasing  $n$ .

Figure 2 provides a comprehensive visual representation of the performance of MLE for the parameters  $q$ ,  $k$ , and  $\lambda$  of the  $q$ -Weibull distribution under various conditions. The panels illustrate how MSE, Bias<sup>2</sup>, and MedAE evolve as the sample size increases and under different parameter constraints.

- Panels (a), (b), and (c): These show the estimation performance when  $q$ ,  $k$ , and  $\lambda$  are independently estimated while the other parameters are fixed. As expected, larger sample sizes lead to more accurate estimates, both MSE and Bias<sup>2</sup> drop noticeably, and the MedAE follows suit, showing that the estimates become not only more precise but also more robust.
- Panels (d), (e), and (f): show what happens when we fix two parameters and estimate just one. Compared to estimating each parameter independently, the error metrics here are lower. This makes sense: with fewer parameters to estimate, the model has more stability.
- Panels (g), (h) and (i): tackle the hardest scenario, estimating all three parameters at once, with no constraints. In this case, the error metrics are higher, which is unsurprising given the increased complexity of estimating multiple parameters simultaneously.

Overall, these results underscore how both sample size and the number of freely estimated parameters influence the accuracy and reliability of MLE for the  $q$ -Weibull distribution. They also offer a clear look at the inherent trade-offs in parameter estimation.

Table 3 summarizes the outcomes of a parameter estimation study conducted across three distinct cases. For each case, the table presents the estimated parameter value, along with its standard deviation (Std), mean absolute error (MAE), and the corresponding confidence interval. The table shows that the estimates of the parameters are generally more accurate when more parameters are fixed. For

example, the estimates of  $q$  are more accurate when  $k$  and  $\lambda$  are fixed, and the estimates of  $k$  are more accurate when  $q$  and  $\lambda$  are fixed. This is because fixing parameters reduces the number of degrees of freedom and makes the estimation problem more tractable. The table also shows that the confidence intervals of the estimates are generally wider when more parameters are fixed. This is because fixing parameters reduces the amount of information available about the parameters, which makes it more difficult to estimate their values accurately.

Table 3 suggests that fixing parameters can be an effective way to improve the accuracy of estimates of distribution parameters. However, it is important to note that fixing parameters can also reduce the width of the confidence intervals of the estimates. Therefore, it is important to choose the method of estimation that is most appropriate for the specific problem at hand.

### Metropolis-Hastings (MH) Algorithm for $q$ -Weibull Distribution Parameters

This section will investigate the effectiveness of the MH algorithm in estimating the parameters of the  $q$ -Weibull distribution. The MH algorithm will be implemented and compared to MLE in terms of estimation accuracy and computational efficiency. The performance of the MH algorithm will be evaluated under various sample sizes and parameter values.

To demonstrate and contrast the effectiveness of the previously mentioned methods, random samples of sizes  $n = 25, 50, 100,$  and  $200$  were generated from the  $q$ -Weibull distribution. This approach accommodates varying data set sizes, encompassing small, medium, and large datasets.

The value of the analogue parameter  $q$  was set to 0.25 and 0.5, while the shape parameter  $k$  was held constant at 1 and 2. The scale parameter  $\lambda$  was also fixed at 2 and 1. We generated  $M=1000$  distinct artificial datasets and

**Table 3.** Estimation results for different cases

Cases	Fixed parameters	Estimate	Std	MAE	CI
Case 1	$k$ and $\lambda$	$\hat{q} = 0.4487$	0.1937	0.0513	[0.3676 0.5298]
	$q$ and $\lambda$	$\hat{k} = 0.9714$	0.0137	0.0286	[0.8723 1.0802]
	$q$ and $k$	$\hat{\lambda} = 1.9569$	0.0444	0.0431	[0.9653 3.0086]
Case 2	$q$	$\hat{k} = 0.9534$	0.0174	0.0466	[0.8054 1.1539]
		$\hat{\lambda} = 1.9246$	0.0093	0.0754	[0.8024 3.0050]
	$k$	$\hat{q} = 0.4420$	0.1303	0.0580	[-0.4584 1.5982]
		$\hat{\lambda} = 1.8260$	0.0113	0.1740	[-0.4424 4.0896]
$\lambda$	$\hat{q} = 0.5726$	0.1599	0.0726	[0.4803 0.6649]	
	$\hat{k} = 1.0946$	0.1024	0.0946	[1.0116 1.1776]	
Case 3	-	$\hat{q} = 0.5542$	0.1345	0.0541	[0.1682 0.8571]
		$\hat{k} = 0.9006$	0.0295	0.0995	[0.7593 1.0562]
		$\hat{\lambda} = 1.8650$	0.0291	0.1350	[1.0727 2.6724]

estimated the parameters using MLE, IMH, and RWM. Hyperparameter values were fixed at  $q_1 = q_2 = k_1 = k_2 = \lambda_1 = \lambda_2 = 0.1$  to achieve a prior distribution with a substantial variance.

For the  $m^{th}$  generated artificial dataset, we apply IMH and RWM, with fixed iterations  $L = 55000$  and a burn-in of  $B = 5000$ . With these settings, the estimates  $(\tilde{q}^{(m)}, \tilde{k}^{(m)}, \tilde{\lambda}^{(m)})$  for  $(q, k, \lambda)$  are obtained by averaging the values generated. In other words:

$$\tilde{q}^{(l)} = \frac{1}{L} \sum_{l=1}^L q^{(m)}, \quad \tilde{k}^{(m)} = \frac{1}{L} \sum_{l=1}^L k^{(l)}, \quad \text{and} \quad \tilde{\lambda}^{(m)} = \frac{1}{L} \sum_{l=1}^L \lambda^{(l)}$$

for  $m = 1, \dots, M$ . The results are presented using the average of the  $M$  parameter estimates, denoted by  $\hat{q}, \hat{k}$  and  $\hat{\lambda}$ .

Tables 3 and 4 display the mean estimates (Est.) and corresponding Standard deviations (Std), Mean Absolute Errors (MAE), and Confidence Interval (CI) values organized by method, considering  $q$  values of 0.25 and 0.5,  $k = 2, 1$  and  $\lambda = 1, 2$ , respectively. Additionally, the percentage of accepted values (%acc.) for the IMH and RWM methods is presented in these tables. Notably, the tables highlight in bold font the smaller standard deviations, mean absolute errors, and widths of confidence intervals for each sample size.

In the analysis of the presented Tables 3 and 4, a noteworthy observation is that the IMH and RWM methods appear to emerge as the most accurate and precise when compared to MLE. This conclusion is based on several

indicators across different sample sizes and true parameter values.

The results are clear: IMH and RWM are no slouches. They deliver estimates that are just as accurate as MLE (sometimes even better) with standard deviations that stay in check and MAE that's right in line. Their confidence intervals may be a tad wider, but they still do their job, covering the true parameters every time. This flips the script on the idea that MLE is always superior. Here, IMH and RWM step up, proving they're more than capable of delivering accurate, precise estimates across different sample sizes and parameter settings.

### APPLICATION

Within this section, we assess the efficacy of MLE, IMH, and RWM on two datasets that are publicly accessible. The dataset that serves as the focal point of this study, as detailed in Table 9, was originally introduced in [24]. Widely recognized and frequently employed in statistical analyses. This dataset consists of real-world data pertaining to the fatigue failure times of N 304 6061-T6 aluminium coupons. These coupons were subjected to oscillation at 18 cycles per second (cps) under two distinct constant levels of maximum stress per cycle: 31,000 psi for 1 second (1s) and 26,000 psi for 2 seconds (2s). Each stress level produced a comprehensive set of failure data, with  $n_1 = 101$  failures observed at 31,000 psi and  $n_2 = 102$  failures observed at 26,000 psi, respectively [6]. The outcomes are derived utilizing the Matlab programming language.

**Table 3.** Average of estimates, Std, MAE and CI by method ( $q = 0.25, k = 1, \lambda = 2$ )

Method		Statistic			Sample size											
					25			50			100			200		
		$\hat{q}$	$\hat{k}$	$\hat{\lambda}$	$\hat{q}$	$\hat{k}$	$\hat{\lambda}$	$\hat{q}$	$\hat{k}$	$\hat{\lambda}$	$\hat{q}$	$\hat{k}$	$\hat{\lambda}$			
MLE	Est.	0.2617	0.9000	1.9604	0.25823	0.9234	2.0377	0.3415	0.9000	1.9375	0.26254	0.9001	2.0171			
	Std	0.0001	0.0007	0.0002	0.0010	0.0009	0.0001	0.0012	0.0006	0.0001	0.0001	0.0009	0.0002			
	MAE	0.3111	0.1000	0.0396	1.7500	0.0999	0.0377	2.0356	0.0915	0.1000	0.0625	1.7500	0.0999			
	CI	[0.1254, 1.5346]	[0.5752, 1.2249]	[0.2743, 4.1951]	[0.2134, 0.2918]	[0.7208, 1.0794]	[1.7208, 2.3794]	[-0.2141, 0.8970]	[0.7464, 1.0537]	[0.8511, 3.0239]	[0.2468, 0.2756]	[0.8121, 0.9881]	[1.9854, 2.1761]			
IMH	Est.	0.2400	0.8995	1.3835	0.2591	1.0167	1.8199	0.2566	1.0003	1.9832	0.2523	1.0530	2.0711			
	Std	0.0348	0.0133	0.3639	0.0317	0.0183	0.6769	0.0013	0.0317	0.1570	0.0020	0.0034	0.0365			
	MAE	0.0099	0.1005	0.6165	0.0091	0.0167	0.1801	0.0066	0.0003	0.0169	0.0023	0.0530	0.0711			
	CI	[0.2154, 0.2646]	[0.8901, 0.9089]	[1.1262, 1.6408]	[0.2238, 0.2851]	[1.0055, 1.0378]	[1.0385, 2.2246]	[0.2553, 0.2579]	[0.9664, 1.0292]	[1.8791, 2.1637]	[0.2501, 0.2540]	[1.0497, 1.0566]	[2.0311, 2.1028]			
	% acc	0.0072	0.0018	0.0018	0.0055	0.0054	0.0036	0.8076	0.0390	0.0885	0.8166	0.6323	0.6875			
RWM	Est.	0.2672	0.9529	1.9026	0.2581	1.0119	1.7695	0.2579	1.0335	2.2098	0.2514	1.0544	2.0613			
	Std	0.0065	0.0366	0.0272	0.0553	0.0791	0.8563	0.0037	0.0327	0.4083	0.0014	0.0047	0.0658			
	MAE	0.0172	0.0471	0.0974	0.0081	0.0119	0.2305	0.0079	0.0335	0.2098	0.0014	0.0544	0.0613			
	CI	[0.2627, 0.2718]	[0.9270, 0.9787]	[1.8834, 1.9218]	[0.2094, 0.3183]	[0.9497, 1.1009]	[0.7902, 2.3774]	[0.2547, 0.2620]	[1.0001, 1.0654]	[1.7554, 2.546]	[0.2504, 0.2529]	[1.0514, 1.0598]	[2.0129, 2.1363]			
	% acc	0.0072	0.0018	0.0001	0.0036	0.0018	0.0036	0.8060	0.0335	0.1062	0.8147	0.6292	0.6852			

**Table 4.** Average of estimates, Std, MAE and CI by method ( $q = 0.5, k = 2, \lambda = 1$ )

Method		Statistic Sample size											
		25			50			100			200		
		$\hat{q}$	$\hat{k}$	$\hat{\lambda}$	$\hat{q}$	$\hat{k}$	$\hat{\lambda}$	$\hat{q}$	$\hat{k}$	$\hat{\lambda}$	$\hat{q}$	$\hat{k}$	$\hat{\lambda}$
MLE	Est.	0.2434	1.8005	1.0233	0.4811	1.8002	0.9621	0.4786	1.8001	0.9792	0.4062	1.800	0.9864
	Std	0.3025	0.0001	0.0273	0.0067	0.0026	0.0001	0.1800	0.0004	0.0169	0.1023	0.0002	0.0062
	MAE	0.2566	0.1995	0.0234	0.0189	0.1998	0.0379	0.0214	0.1999	0.0208	0.0938	0.1999	0.0136
	CI	[-0.2540, 1.4416]	[1.0857, 2.5294]	[0.4514, 1.5906]	[-0.1785, 1.1243]	[1.3658, 2.2435]	[0.6102, 1.3148]	[-2.0702, 3.2515]	[-0.1746, 3.7901]	[-0.9432, 2.9254]	[0.0922, 0.8648]	[1.5457, 2.0544]	[0.7573, 1.2243]
IMH	Est.	0.4955	2.1427	1.0138	0.50128	2.0597	1.0266	0.5088	2.0138	1.0424	0.5028	2.0166	0.9941
	Std	0.0658	0.1562	0.0045	0.0033	0.0063	0.0217	0.0017	0.0062	0.0168	0.0037	0.0037	0.0149
	MAE	0.0471	0.1427	0.0138	0.0013	0.0597	0.0266	0.0088	0.0138	0.0424	0.0028	0.0166	0.0059
	CI	[0.4336, 0.5625]	[1.9635, 2.2652]	[0.9745, 1.0637]	[0.4568, 0.5027]	[2.0532, 2.0792]	[1.0175, 1.0506]	[0.5065, 0.5118]	[2.0154, 2.0235]	[1.0236, 1.0604]	[0.5001, 0.5054]	[2.0140, 2.0192]	[0.9836, 1.0047]
	% acc	0.4341	0.0065	0.0392	0.5469	0.4559	0.6517	0.6373	0.7425	0.804	0.6963	0.8310	0.8601
RWM	Est.	0.5169	2.2353	1.2019	0.5025	2.0669	1.043	0.5141	2.0157	1.0384	0.5070	2.0252	1.0045
	Std	0.0518	0.4306	0.3391	0.0012	0.0146	0.0287	0.0026	0.0069	0.0062	0.0032	0.0005	0.0149
	MAE	0.0169	0.2353	0.2019	0.0025	0.0669	0.0430	0.0141	0.0157	0.0384	0.0070	0.0252	0.0045
	CI	[0.4725, 0.5702]	[1.9171, 2.7254]	[0.9382, 1.5804]	[0.5002, 0.5095]	[2.0645, 2.0852]	(1.02, 1.08)	(0.51, 0.52)	(2.01, 2.02)	(1.03, 1.04)	[0.5048, 0.5093]	[2.0248, 2.0255]	[0.9939, 1.0151]
	% acc	0.4213	0.0060	0.0714	0.5406	0.4594	0.6458	0.6382	0.7413	0.8026	0.6964	0.8327	0.8612

To evaluate the performance of methods, we examine the Root Mean Square Error (RMSE) concerning the empirical distribution function, as expressed by:

$$RMSE = \sqrt{\frac{1}{n} \sum_{i=1}^n [\hat{F}(x_i) - F(x_i)]^2}$$

where,  $\hat{F}(x)$  is derived by substituting the estimates of parameters  $q, k$  and  $\lambda$  obtained through each respective method. Meanwhile,  $F(x_i)$  represents the empirical distribution function obtained from Kaplan-Meier estimates for each  $i = 1, \dots, n$ . The method exhibiting the lowest RMSE is considered the most effective among the candidate methods for fitting the model.

Tables 6 and 7 summarize the parameter estimates and RMSE values for various distributions, including Fréchet, Ishita, Birnbaum–Saunders, Weibull, and  $q$ -Weibull, applied to the fatigue life data at stress levels 31,000 psi and 26,000 psi, respectively. Across both stress levels, the  $q$ -Weibull model came out on top, with RWM consistently delivering the lowest RMSE among all the distributions we tested. This really underscores how robust and reliable the  $q$ -Weibull model is for capturing fatigue life data, especially when stacked against the alternatives.

Figures 3 and 4 compare survival functions for fatigue life data at two stress levels (31,000 psi and 26,000 psi) across several distributions and estimation methods. The RWM and IMH curves are nearly indistinguishable, confirming their consistency. For clarity, we've focused on the most informative comparisons. The Kaplan-Meier step

**Table 6.** Parameter estimates and RMSE by method for the indicated models for the fatigue life data at stress level 31,000 psi.

Parameter	Fréchet	Ishita	Birnbaum–Saunders	Weibull	$q$ -Weibull		
					MLE	IMH	RWM
$\hat{q}$	-	-	-	-	0.86643	0.88341	0.86764
$\hat{k}$	5.0575	422.22	131.819	6.07343	7.08523	6.74273	6.87903
$\hat{\lambda}$	120.7822	-	0.170385	143.167	146.06946	146.07199	148.42818
RMSE	0.054699	0.43237	0.18215	0.04053	0.03287	0.02596	0.02429

**Table 7.** Parameter estimates and RMSE by method for the indicated models for the fatigue life data at stress level 26,000 psi.

Parameter	Fréchet	Ishita	Birnbbaum–Saunders	Weibull	q-Weibull		
					MLE	IMH	RWM
$\hat{q}$	-	-	-	-	0.82207	0.87516	0.853304
$\hat{k}$	5.5549	105.55	392.762	7.0075	6.602151	6.852165	6.806042
$\hat{\lambda}$	361.3133	-	0.161448	424.3782	435.30069	432.82873	432.59715
RMSE	0.053135	0.5003	0.017363	0.02782	0.024201	0.024981	0.024061

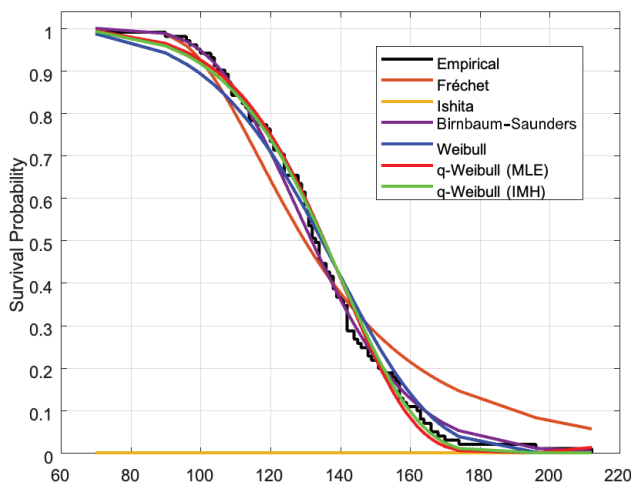


**Figure 3.** Survival probability estimates for fatigue life data at stress levels 31,000 psi, using MLE, IMH, and the Weibull model. Bayesian methods (IMH) show closer alignment with empirical data, reflected in lower RMSE values.

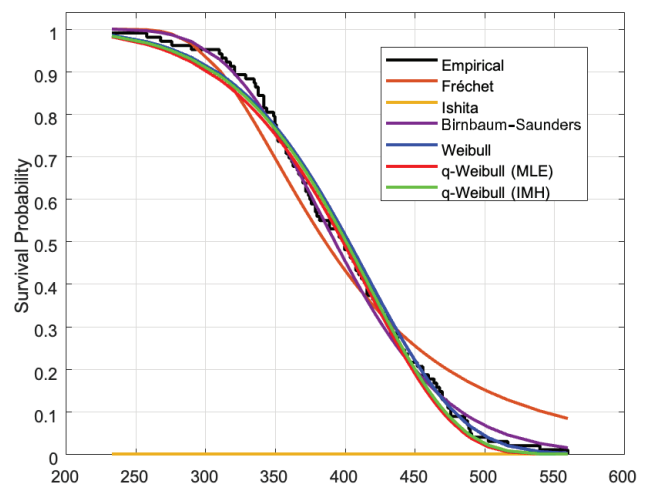


**Figure 4.** Survival probability estimates for fatigue life data at stress levels 26,000 psi, using MLE, IMH, and the Weibull model. Bayesian methods (IMH) show closer alignment with empirical data, reflected in lower RMSE values.

function provides the empirical benchmark. The  $q$ -Weibull model, particularly when estimated with Bayesian methods like IMH. It aligns with the Kaplan-Meier curve better than any other distribution, indicating a superior fit.

This showcases the advantage of Bayesian estimation: leveraging prior information and iterative learning to better capture the data. The other distributions (Fréchet, Ishita, Birnbbaum–Saunders, and Weibull) perform reasonably well but show noticeable deviations, especially in the tails. These deviations highlight the limitations of traditional frequentist methods and other fixed-form distributions in capturing complex survival patterns. Together, these figures highlight just how well the  $q$ -Weibull model and Bayesian methods perform, particularly for datasets where survival behaviour is variable or follows a non-linear path. By incorporating prior distributions and employing iterative sampling techniques, Bayesian methods achieve a closer alignment with empirical observations, making them especially effective for real-world reliability analysis. This comparison further underscores just how robust and adaptable

the  $q$ -Weibull model really is it consistently captures complex survival dynamics across a range of scenarios.

Figures 5 and 6 show the traceplots, ergodic means, and autocorrelation times for the parameters  $q$ ,  $k$  and  $\lambda$  under IMH and RWM, respectively. These results come from the fatigue data at 31,000 psi (the corresponding plots for 26,000 psi are in the Appendix Table 1, Figures 7 and 8).

In stark contrast, IMH presents a scenario characterized by inadequate mixing and unsatisfactory autocorrelation and stability in terms of ergodic mean. These observations, coupled with the consideration of the RMSE value, collectively point towards the superior performance of RWM in comparison to MLE for these datasets. Conversely, IMH falls short in terms of performance, as indicated by its suboptimal mixing and inadequate autocorrelation and stability for ergodic mean.

Table 8 presents a comparative summary of the three estimation Maximum Likelihood Estimation (MLE) Independent Metropolis-Hastings (IMH) and Random Walk Metropolis (RWM), based on the results obtained in our study.

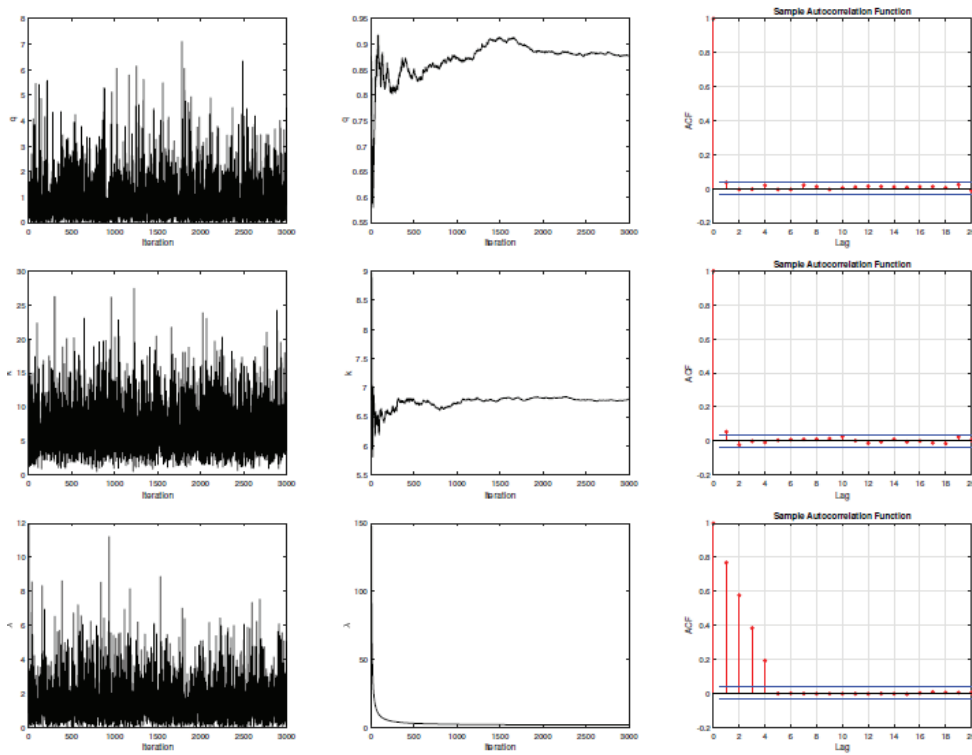


**Figure 5.** Traceplots, ergodic mean and Autocorrelation by IMH of parameters  $q$ ,  $k$  and  $\lambda$  for fatigue life data at the stress levels 31000 psi.

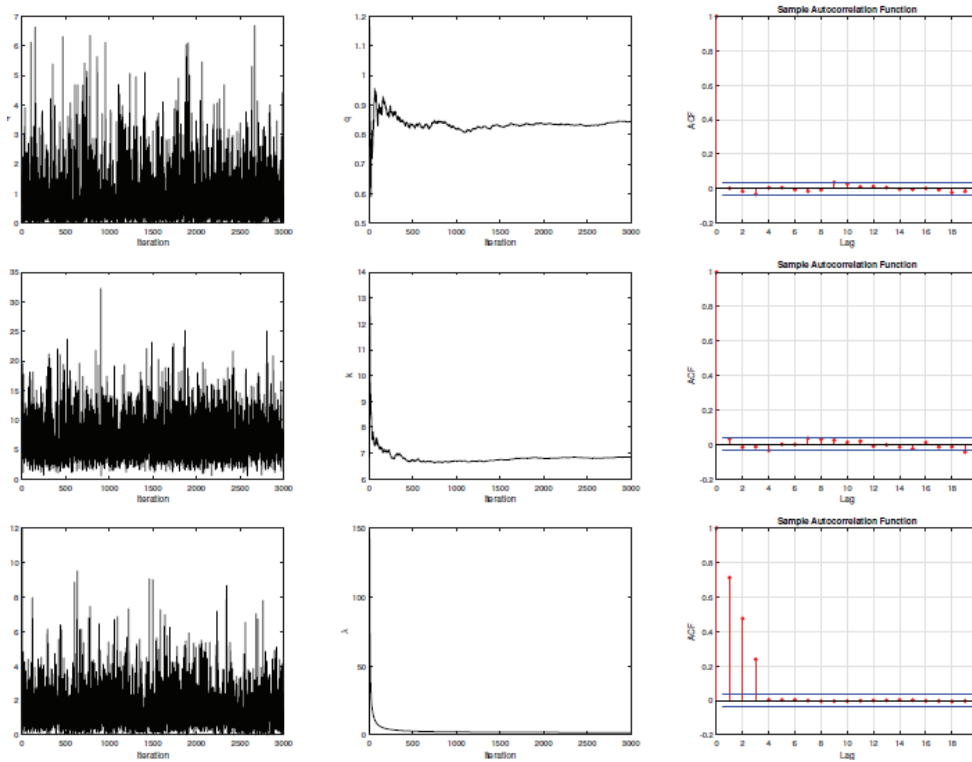


**Figure 6.** Traceplots, ergodic mean and Autocorrelation by RWM of parameters  $q$ ,  $k$  and  $\lambda$  for fatigue life data at the stress levels 31000 psi.

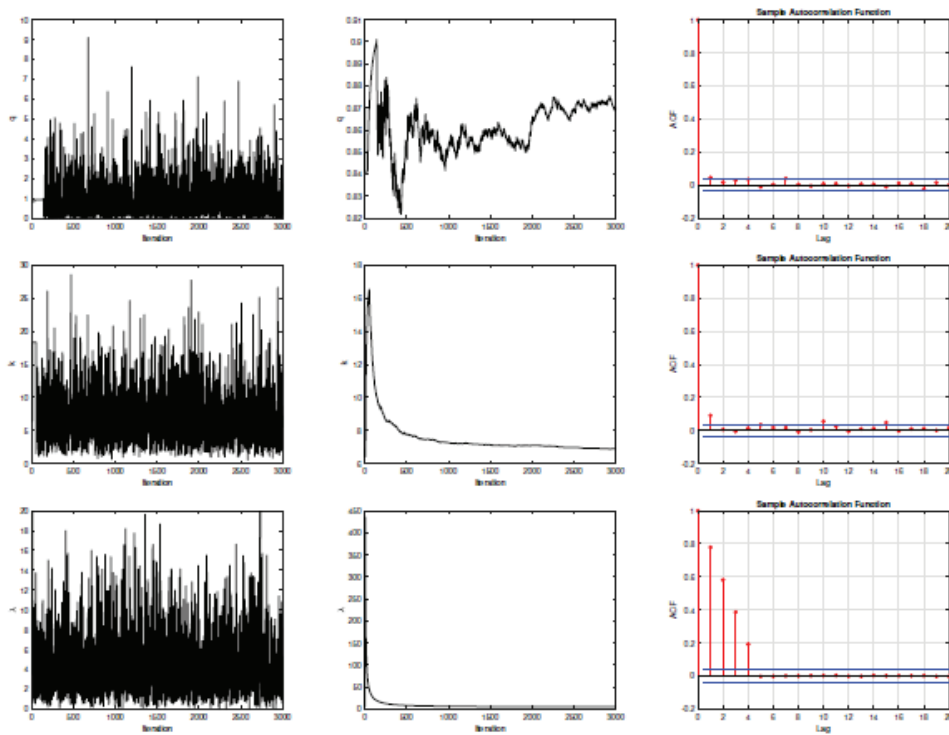


**Figure 7.** Traceplots, ergodic mean and autocorrelation by IMH of parameters  $q$ ,  $k$  and  $\lambda$  for fatigue life data at the stress levels 26000 psi.

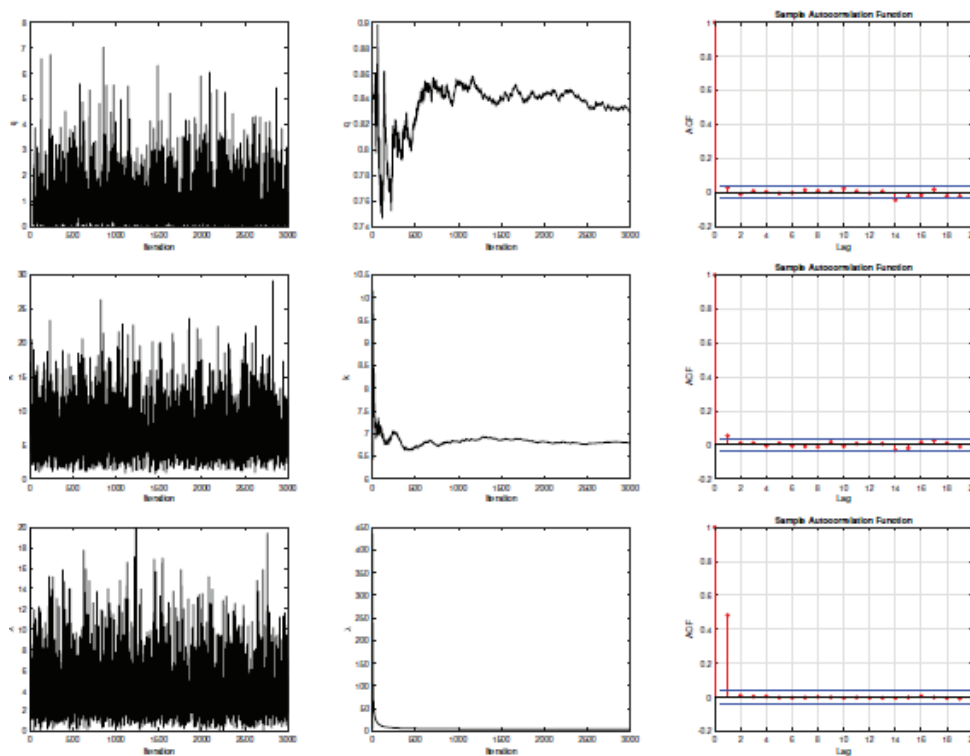


**Figure 8.** Traceplots, ergodic mean and Autocorrelation by RWM of parameters  $q$ ,  $k$  and  $\lambda$  for fatigue life data at the stress levels 26000 psi.

**Table 8.** Comparison of MLE, metropolis-hastings (MH), independent metropolis-hastings (IMH), and random walk metropolis (RWM) methods based on results

Method	Performance	Advantages	Limitations
MLE	Competitive performance for small datasets; moderate RMSE in real-data results.	Straightforward implementation; widely used and well-understood approach in parameter estimation.	May yield less accurate estimates than Bayesian methods (IMH, RWM), especially in the context of large or complex datasets.
IMH	Good accuracy and variability for larger datasets, but mixing and autocorrelation could be better for some parameters.	Effective when the candidate distribution closely matches the posterior; leads to fewer rejections than MH.	Performs well only if the proposal distribution is carefully chosen; otherwise, the ergodic means can become unstable.
RWM	Best performance overall: lowest RMSE for both simulation and real-data results; robust convergence.	Excellent mixing properties, efficient exploration, stable results across sample sizes and stress levels.	Requires careful tuning of step size (proposal variance); large or small values impact convergence.

## CONCLUSION

This study bridges critical gaps in the application of the  $q$ -Weibull distribution by introducing and evaluating Bayesian computational methods for parameter estimation. We compared three methods: MLE, Independent Metropolis-Hastings, and Random Walk Metropolis. Using Monte Carlo simulations and real-world datasets, we evaluated them on standard deviation, mean absolute errors, and confidence intervals.

The  $q$ -Weibull distribution, estimated with Bayesian methods, consistently outperformed alternatives like Fréchet, Ishita, Birnbaum–Saunders, and Weibull. RWM, in particular, stood out, it had the lowest RMSE and matched the empirical survival probabilities better than any other method. This shows just how robust and flexible the  $q$ -Weibull is, and it makes a strong case for MCMC methods as viable alternatives to traditional approaches.

Bayesian methods, particularly IMH and RWM, are computationally intensive. MCMC algorithms run on iterations, which means they demand significant time and computing power, especially when datasets are large. It's a trade-off, but one we think is justified by the gains in accuracy and robustness, even if it can be a hurdle for some real-world applications. The source code employed in both the simulation study and practical applications was implemented in Matlab software.

## AUTHORSHIP CONTRIBUTIONS

Authors equally contributed to this work.

## DATA AVAILABILITY STATEMENT

The authors confirm that the data that supports the findings of this study are available within the article. Raw data that support the finding of this study are available from the corresponding author, upon reasonable request.

## CONFLICT OF INTEREST

The author declared no potential conflicts of interest with respect to the research, authorship, and/or publication of this article.

## ETHICS

There are no ethical issues with the publication of this manuscript.

## STATEMENT ON THE USE OF ARTIFICIAL INTELLIGENCE

Artificial intelligence was not used in the preparation of the article.

## REFERENCES

- [1] Yu J. Prediction of survival time for breast cancer patients. Dalhousie University, Halifax, Nova Scotia 2022.
- [2] Barraza-Contreras JM, Piña-Monarez MR, Molina A. Fatigue-life prediction of mechanical element by using the Weibull distribution. *Appl Sci* 2020;10:6384. [\[CrossRef\]](#)
- [3] Sarkar A, Deep S, Datta D, Vijaywargiya A, Roy R, Phanikanth VS. Weibull and generalized extreme value distributions for wind speed data analysis of some locations in India. *KSCE J Civ Eng* 2019;23:3476–3492. [\[CrossRef\]](#)
- [4] Wiradinata T, Graciella F, Tanamal R, Soekamto YS, Saputri TRD. Post-pandemic analysis of house price prediction in Surabaya: a machine learning approach. *J Southwest Jiaotong Univ* 2022;57:562–573. [\[CrossRef\]](#)
- [5] Sadok I, Zribi M. Image restoration using Weibull particle filters. In: 2022 4th International Conference on Pattern Analysis and Intelligent Systems (PAIS); 2022 Oct. p. 1–6. IEEE. [\[CrossRef\]](#)

- [6] D'Anna G, Giorgio M, Riccio A. Estimating fatigue life of structural components from accelerated data via a Birnbaum-Saunders model with shape and scale stress dependent parameters. *Procedia Eng* 2016;167:10–17. [\[CrossRef\]](#)
- [7] Jose KK, Naik SR. On the q-Weibull distribution and its applications. *Commun Stat Theory Methods* 2009;38:912–926. [\[CrossRef\]](#)
- [8] Picoli Jr S, Mendes RS, Malacarne LC. q-exponential, Weibull, and q-Weibull distributions: an empirical analysis. *Physica A Stat Mech its Appl* 2003;324:678–688. [\[CrossRef\]](#)
- [9] Vuorenmaa T. A q-Weibull autoregressive conditional duration model and threshold dependence. University of Helsinki, RUESG and HECER 2006;117:1–61.
- [10] Sadok I. On the q-Rayleigh distribution and its applications. *Reliab Theory Appl* 2024;19:588–602.
- [11] Assis EM, Borges EP, Vieira de Melo SA. Generalized q-Weibull model and the bathtub curve. *Int J Qual Reliab Manag* 2013;30:720–736. [\[CrossRef\]](#)
- [12] Douini H, Sadok I. A study on statistical properties of a new class of q-Fréchet distribution. *Math Appl Sci Eng* 2020;1–23.
- [13] Costa UMS, Freire VN, Malacarne LC, Mendes RS, Picoli Jr S, De Vasconcelos EA, et al. An improved description of the dielectric breakdown in oxides based on a generalized Weibull distribution. *Physica A Stat Mech its Appl* 2006;361:209–215. [\[CrossRef\]](#)
- [14] Al-Essa LA, Saboor A, Tahir MH, Khan S, Jamal F, Elhassanein A. Bivariate q-generalized extreme value distribution: a comparative approach with applications to climate related data. *Heliyon* 2024;10:8. [\[CrossRef\]](#)
- [15] Agrawal S, Vats D, Łatuszyński K, Roberts GO. Optimal scaling of MCMC beyond Metropolis. *Adv Appl Prob* 2023;55:492–509. [\[CrossRef\]](#)
- [16] Zribi M, Sadok I, Marhaba B. Kernel-diffeomorphism Bayesian bootstrap filter to reduce speckle noise on SAR images. *Comput Stat* 2025;40:3613–3643. [\[CrossRef\]](#)
- [17] Blei DM, Kucukelbir A, McAuliffe JD. Variational inference: a review for statisticians. *J Am Stat Assoc* 2017;112:859–877. [\[CrossRef\]](#)
- [18] Chib S, Greenberg E. Understanding the Metropolis-Hastings algorithm. *Am Stat* 1995;49:327–335. [\[CrossRef\]](#)
- [19] Saraiva EF, Suzuki AK. Bayesian computational methods for estimation of two-parameters Weibull distribution in presence of right-censored data. *Chilean J Stat* 2017;8:25–43.
- [20] Xu M, Droguett EL, Lins ID, das Chagas Moura M. On the q-Weibull distribution for reliability applications: an adaptive hybrid artificial bee colony algorithm for parameter estimation. *Reliab Eng Syst Saf* 2017;158:93–105. [\[CrossRef\]](#)
- [21] Sadok I. Non-informative Bayesian dispersion particle filter. *J Innov Appl Math Comput Sci* 2023;3:173–189.
- [22] Sadok I, Zribi M, Masmoudi A. Non-informative Bayesian estimation in dispersion models. *Hacetatepe J Math Stat* 2023;53:251–268. [\[CrossRef\]](#)
- [23] Hastings WK. Monte Carlo sampling methods using Markov chains and their applications. 1970;57:97–109. [\[CrossRef\]](#)
- [24] Birnbaum ZW, Saunders SC. Estimation for a family of life distributions with applications to fatigue. *J Appl Prob* 1969;6:328–347. [\[CrossRef\]](#)
- [25] Méndez-González LC, Rodríguez-Picón LA, González-Hernández IJ, Pérez-Olguín IJC, Quezada-Carreón AE. The Fréchet-Chen distribution and its applications to reliability analysis of electronic devices. Preprints 2024. doi: 10.20944/preprints202409.1956.v12024. [\[CrossRef\]](#)
- [26] Hassan A, Dar SA, Para BA. A new generalization of Ishita distribution: properties and applications. *J Appl Prob Stat* 2019;13:53–67.
- [27] Sadok I, Masmoudi A, Zribi M. Integrating the EM algorithm with particle filter for image restoration with exponential dispersion noise. *Commun Stat Theory Methods* 2023;52:446–462. [\[CrossRef\]](#)
- [28] Sadok I, Masmoudi A. New parametrization of stochastic volatility models. *Commun Stat Theory Methods* 2022;51:1936–1953. [\[CrossRef\]](#)

**Appendix Table 1.** Failure data collected

<b>Failure data collected at 31000 psi</b>																
70	90	96	97	99	100	103	104	104	105	107	108	108	108	109	109	112
112	113	114	114	114	116	119	120	120	120	121	121	123	124	124	124	124
124	128	128	129	139	130	130	130	131	131	131	131	131	132	132	132	133
134	134	134	134	134	136	136	137	138	138	138	139	139	141	141	142	142
142	142	142	142	144	144	145	146	148	148	149	151	151	152	155	156	157
157	157	157	158	159	162	163	163	164	166	166	168	170	174	196	212	
<b>Failure data collected at 26000 psi</b>																
233	258	268	276	290	310	312	315	318	321	321	329	335	336	338	338	342
342	342	344	349	350	350	351	351	352	352	356	358	358	360	362	363	366
367	370	370	372	372	374	375	376	379	379	380	382	389	389	395	396	400
400	400	403	404	406	408	408	410	412	414	416	416	416	420	422	423	426
428	432	432	433	433	437	438	439	439	443	445	445	452	456	456	460	464
466	468	470	470	473	474	476	476	486	488	489	490	491	503	517	540	560